



Campagnolo, P., Gormley, A. J., Chow, L. W., Guex, A. G., Parmar, P. A., Puetzer, J. L., Steele, J. A. M., Breant, A., Madeddu, P., & Stevens, M. M. (2016). Pericyte Seeded Dual Peptide Scaffold with Improved Endothelialization for Vascular Graft Tissue Engineering. *Advanced Healthcare Materials*, 5(23), 3046-3055.  
<https://doi.org/10.1002/adhm.201600699>

Peer reviewed version

Link to published version (if available):  
[10.1002/adhm.201600699](https://doi.org/10.1002/adhm.201600699)

[Link to publication record in Explore Bristol Research](#)  
PDF-document

This is the author accepted manuscript (AAM). The final published version (version of record) is available online via Wiley at <http://onlinelibrary.wiley.com/doi/10.1002/adhm.201600699/full>. Please refer to any applicable terms of use of the publisher.

## University of Bristol - Explore Bristol Research

### General rights

This document is made available in accordance with publisher policies. Please cite only the published version using the reference above. Full terms of use are available:  
<http://www.bristol.ac.uk/red/research-policy/pure/user-guides/ebr-terms/>

**Article type: Full Paper**

**Pericyte seeded dual peptide scaffold with improved endothelialization for vascular graft tissue engineering**

*Paola Campagnolo, Adam J Gormley, Lesley W Chow, Anne Géraldine Guex, Paresh A Parmar, Jennifer L Puetzer, Joseph AM Steele, Alexandre Breant, Paolo Madeddu, Molly M Stevens<sup>\*</sup>.*

Dr Paola Campagnolo 1, Dr Adam J Gormley 1, Dr Lesley W Chow 1, Dr Anne Géraldine Guex 1,2 Dr Paresh A Parmar 1, Dr Jennifer L Puetzer 1, Dr Joseph AM Steele 1, Mr Alexandre Breant 1, Prof Paolo Madeddu 3, Prof Molly M Stevens 1.

1 Department of Materials, Department of Bioengineering and Institute of Biomedical Engineering,

Imperial College London, Royal School of Mines, Prince Consort Rd,  
SW7 2AZ, London, UK

2 National Heart and Lung Institute, Imperial College London, 435 Du Cane Road, W12 0NN, London, UK

3 Bristol Heart Institute, University of Bristol, Bristol Royal Infirmary,  
Upper Maudlin St,  
BS2 8HW, Bristol, UK

Keywords: tissue engineered vascular graft, electrospinning, biofunctionalization, endothelialization, pericytes

## **Abstract**

The development of synthetic vascular grafts for coronary artery bypass is challenged by insufficient endothelialization, which exposes to the risk of thrombosis, and lack of native cellular constituents, which favours pathological remodelling. Here, an bifunctional electrospun poly( $\epsilon$ -caprolactone) (PCL) scaffold with potential for synthetic vascular graft applications is presented. This scaffold incorporates two tethered peptides: the osteopontin-derived peptide (Adh) on the ‘luminal’ side and a heparin-binding peptide (Hep) on the ‘abluminal’ side. Additionally, the ‘abluminal’ side of the scaffold is seeded with saphenous vein-derived pericytes (SVPs) as a source of pro-angiogenic growth factors. The Adh peptide significantly increase endothelial cell adhesion, while the Hep peptide promote accumulation of vascular endothelial growth factor (VEGF) secreted by SVPs. SVPs increase endothelial migration both in a transwell assay and a modified scratch assay performed on the PCL scaffold. Seeding of SVPs on the ‘abluminal’/Hep side of the scaffold further increase endothelial cell density, indicating a combinatory effect of the peptides and pericytes. Lastly, SVP-seeded scaffolds are preserved by freezing in a xeno-free medium, maintaining good cell viability and function. In conclusion, this engineered scaffold combines patient-derived pericytes and spatially organized functionalities, which synergistically increase endothelial cell density and growth factor retention.

## **1. Introduction**

According to the World Health Organization, coronary artery disease is the leading cause of death and disability in the world. Autologous vascular bypass is a common intervention aimed at re-establishing blood flow to the cardiac tissue in patients for whom balloon angioplasty and/or stenting are not viable options. However, in patients with vascular complications or requiring multiple bypasses, autologous vessels might not be available or

sufficiently healthy. Tissue engineered vascular grafts (TEVGs) are an attractive alternative to natural vessels. In recent years, many different approaches have been tested both *in vitro* and *in vivo* to implement the design of new TEVG, in particular of small diameter vessels below the critical diameter of 6 mm (for reviews see <sup>[1,2]</sup>). In these approaches, cells are seeded on biodegradable vascular scaffolds prepared with a variety of techniques, including hydrogel self-assembly, particulate-leaching, and electrospinning. In particular, electrospinning of biodegradable materials, such as poly( $\epsilon$ -caprolactone (PCL) has been used extensively to obtain biocompatible vascular scaffolds with tuneable functional properties and suitable mechanical properties.<sup>[3]</sup>

Despite remarkable progress, TEVG design remains a challenge in the field of tissue engineering due to the poor performance of non-natural vessels in terms of thrombosis and long-term patency. Largely, graft failure is associated with delayed and insufficient re-endothelialization of the ‘luminal’ surface which exposes the scaffold surface to the blood stream, leading to platelet activation. In order to reduce the risk of failure, the TEVGs should resist thrombosis while promoting a quick re-endothelialization from the neighbouring vascular tissue.<sup>[4]</sup> Previous studies have demonstrated that the pre-implantation seeding of TEVGs, including ‘luminal’ seeding of endothelial cells, dramatically improves their performance.<sup>[5]</sup> More recent studies suggest that the role of the transplanted cells is mainly to provide the initial stimuli to accelerate recruitment of host cells on to the graft, through the release of growth factors and cytokines promoting endothelial cell migration, before being displaced by the host cells.<sup>[6]</sup> In particular, autologous mesenchymal stem cells (MSCs) have shown remarkable anti-thrombogenic properties,<sup>[7]</sup> as also demonstrated in clinical trials.<sup>[8,9]</sup> The adventitia of large vessels contains clonogenic pericytes, which are now considered the primitive progenitors of MSCs. We have recently set up a Good Manufacturing Practises (GMP)-compliant standard operating procedure (SOP) for isolation and expansion of

pericytes from remnants of saphenous vein grafts used for coronary artery bypass surgery.<sup>[10,11]</sup> Saphenous vein-derived pericytes (SVPs) paracrinally promote endothelial cell proliferation and network formation *in vitro* and improve neoangiogenesis and hemodynamic recovery, when transplanted in models of hindlimb ischemia or myocardial infarction.<sup>[10,12,13]</sup> Additionally, SVPs display a privileged immune-modulatory phenotype and could therefore be used for allogeneic purposes.<sup>[14]</sup> However, the exceptional characteristics of SVPs have never been harnessed for tissue engineering of vascular grafts. In this *in vitro* proof-of-concept study, we present a tissue engineered construct composed of an advanced biomaterial seeded with SVPs to recreate the adventitial niche and provide a source of angiocrine factors promoting the graft endothelialization. We hypothesize that this scaffold will see application in the design of TEVG and we will therefore term the two sides of the scaffold as ‘luminal’ and ‘abluminal’ in relation to their potential positioning within a TEVG.

The PCL scaffold produced to support the SVP growth was designed to present spatially defined functionalities, aimed at enhancing and promoting SVP properties. PCL is a biodegradable and readily processable, FDA approved polymer that can be electrospun alone or blended with other polymers to form small diameter vascular grafts that are mechanically sound and amenable to endothelialization.<sup>[3,15,16]</sup>

We have previously described an advanced electrospinning technique to obtain dual functionalized PCL scaffolds for cartilage repair.<sup>[17]</sup> Applying the same technique, we here created a PCL scaffold presenting a spatially organized distribution of two tethered peptides, an osteopontin derived adhesion (Adh) peptide on the ‘luminal’ side, to favour endothelial cell attachment; and a heparin binding peptide (Hep) on the ‘abluminal’ side, where it is ideally placed to coordinate the pericyte-produced growth factors. The Adh peptide is a cryptic binding motif of osteopontin that is exposed following thrombin cleavage typically observed in vascular damage. Adh binds to integrin  $\alpha 4\beta 1$ <sup>[18]</sup> and  $\alpha 9\beta 1$ <sup>[19]</sup> on endothelial cells

and induces cell adhesion and maturation, when provided as a soluble factor<sup>[20]</sup> or patterned on a surface.<sup>[21]</sup> Furthermore, when conjugated to a PEG based hydrogel, Adh displayed a strong pro-angiogenic activity both *in vitro*<sup>[22]</sup> and *in vivo*.<sup>[22,23]</sup> Importantly, Adh has been shown to reduce macrophage attachment and promote their differentiation towards the reparative phenotype.<sup>[24,25]</sup> The Hep peptide is a small amphiphilic sequence that binds heparin and can improve endothelial cell function and angiogenesis.<sup>[26-29]</sup> As previously demonstrated, the tethering of heparin to vascular scaffolds improves their performance by retaining and presenting growth factors, such as VEGF and FGF2.<sup>[30]</sup> The presence of the Hep peptide on the ‘abluminal’ side of the scaffold will be crucial to capture and release the SVP-produced growth factors over time.

This study describes an original approach to the design of scaffolds aimed at TEVG, enhancing the activity of the patient-derived cells seeded on it by introducing multiple bio-functionalizations aimed at improving endothelial cell adhesion and growth factor availability. Here we focus on the *in vitro* study of the synergistic contribution of the SVP-released factors and tethered functionalities by studying the biological mechanisms underlying the process of re-endothelialization.

## **2. Results**

### **2.1 Scaffold preparation and characterization**

In this study, we characterized a proof-of-concept model of a peptide-functionalized PCL scaffold for tissue engineered vascular graft applications. The spatial organisation of the scaffold was engineered to present osteopontin-derived peptide (Adh) on the ‘luminal’ side and the heparin-binding peptide (Hep) on the ‘abluminal/adventitial’ side (**Figure 1a**). The advanced electrospinning procedure applied allows precise control of the spatial localization of the two peptide-conjugated polymers and the creation of a dual peptide scaffold presenting

two opposing concentrations of the peptides, as shown in **Figure 1b**. The resulting electrospun mats were imaged by SEM, showing the consistency of the fibre morphology between the unconjugated scaffolds and the Hep/Adh scaffold (**Figure 1c** and **Figure S5**). Indeed, the fibre diameters were similarly distributed between different scaffolds (CTL:  $1.40 \pm 0.59 \mu\text{m}$ ; Hep:  $0.82 \pm 0.18 \mu\text{m}$ ; Adh:  $1.20 \pm 0.47 \mu\text{m}$ ; Hep/Adh:  $0.99 \pm 0.39 \mu\text{m}$  and  $1.52 \pm 0.33 \mu\text{m}$  on either side).

## 2.2 Functional activity of conjugated peptides

The capacity of the Hep peptide to bind heparin and retain growth factors was studied by incubating the different PCL scaffolds with FITC-heparin and SVP-released GFP-tagged VEGF. Indeed, Hep-PCL and Hep/Adh -PCL showed increased fluorescence when incubated with FITC heparin compared to the control-PCL, indicating a preferential binding of heparin to the Hep peptide (**Figure 2a**). Furthermore, human SVPs were transfected with a plasmid expressing VEGF in fusion with GFP and incubated with control scaffold, Hep or Hep/Adh-PCL in presence of heparin. Results showed that the retention of SVP-secreted VEGF was highly improved by the Hep peptide (**Figure 2b**). VEGF loaded Hep-conjugated scaffold were also shown to promote endothelial cell density, as compared to unloaded scaffolds and control scaffolds loaded with VEGF (**Figure 2c** and **Figure 2d**).

Next, the presentation and functionality of Adh peptide was tested by plating HUVECs on the different scaffolds. Adhesion of endothelial cells was assessed by measuring the cell density on the scaffold, confirming that Adh-conjugated scaffolds displayed increased endothelial cell number (**Figure 3**).

## 2.3 Cooperative effect of pericyte seeding and scaffold functionalization

We evaluated the combined effect of the conjugation of the peptides to the scaffold and the seeding of the pericytes on the ‘abluminal’/Hep side, by comparing the endothelial cell density in the presence of each factor or their combination.

A non-contact co-culture system of SVPs and HUVECs was created on both control PCL and Hep/Adh scaffolds by seeding the SVPs on the ‘abluminal’/Hep side and the HUVECs on the ‘luminal’/Adh side of the scaffolds. As a control, HUVECs were cultured in absence of SVPs on both types of scaffold. Quantification of endothelial cell nuclei showed that the combination of the presence of pericytes and the conjugates had a significantly higher impact on endothelial coverage, as compared to each of the factors alone (**Figure 4**).

## **2.4 Effect of pericytes on endothelial cell migration**

Pericytes are known to release a plethora of pro-angiogenic factors; hence we hypothesize that SVPs can improve the migration of endothelial cells. This is particularly relevant in the context of vascular grafting to encourage the migration of the endothelial cells from neighbouring vessels and reach the complete endothelialization of the lumen of the implanted scaffolds. Indeed, the transwell migration assay showed that the presence of pericytes in the lower chamber increased the migration of endothelial cells by 2.5 times in the 8 hours timeframe of the assay (**Figure 5a** and **Figure 5b**).

Furthermore, we confirmed an increased wound closure by endothelial cells in a modified scratch assay performed in a co-culture system on PCL where the endothelial monolayer was interrupted by forming a gap with a polydimethylsiloxane (PDMS) mask (**Figure 5c**).

Fluorescence imaging of the whole ‘luminal’ side of the scaffolds indicated increased presence of endothelial cells in the gap of the scaffolds pre-seeded with pericytes the ‘abluminal/Hep’ (**Figure 5d-g**). Quantification of the mean fluorescence within the gap



showed an average increase of  $67.6 \pm 20.8\%$  in endothelial cell density ( $P < 0.05$ ;  $N = 3$ ) in the SVP-seeded scaffolds.

## **2.5 Freezing of pericytes-coated scaffolds**

The effective deployment of the devised scaffold for the development of clinically relevant TEVG is highly dependent on its resilience to freezing/thawing for preservation/delivery purposes. We tested the feasibility of this approach by freezing the SVP-seeded Hep/Adh PCL scaffolds using a cell therapy-approved xeno-free freezing medium and assessing their viability and functionality after thawing. AlamarBlue® assay results showed that the scaffolds thawed after 14 days of freezing could be efficiently recovered and that over 65% of the pericytes were viable (**Figure 6a**). Despite the 50% reduction in SVP cell number (**Figure 6b**), the cells were still adherent (**Figure 6d**) and were able to stimulate EC density to a level comparable to the fresh SVPs (**Figure 6c** and **Figure 6d**). These results indicate the potential for long-term storage of the pre-prepared vascular grafts based on our scaffold.

## **3. Discussion**

In this work we describe how the biomaterial functionality may be integrated with the properties of the cells seeded on it to develop an implemented biomaterial with improved endothelialization properties for TEVG applications. In this proof-of-concept study, we characterized a polymer-based scaffold presenting a dual peptide functionalization, enabling the differential localization of each peptide and therefore recapitulating tissue-like organization. As compared to classical bulk post-fabrication functionalization, our previously reported sequential electrospinning method provides better control and homogeneity of the functionalization distribution,<sup>[17]</sup> which more closely resembles the complexity of the

precisely layered vascular tissue. In particular, we demonstrated that the presentation of the adhesive peptide Adh on the ‘luminal’ side increased endothelial cell attachment and density. These results are in line with the previously reported pro-angiogenic capacity of the Adh peptide both *in vitro* and *in vivo*.<sup>[20-22]</sup> Earlier studies reported that the surface modification of electrospun PCL scaffolds with the ubiquitous cell adhesion peptide RGD accelerated the endothelialization process in rabbit carotid artery graft.<sup>[31]</sup> Of note, the Adh peptide is derived from the enzymatic cleavage of the pro-angiogenic protein osteopontin, typically occurring at the site of vascular damage<sup>[32]</sup> and is therefore preferentially recognized by endothelial cell expressed integrins, limiting the anchorage of inflammatory cells.<sup>[22,24,25]</sup>

The versatile method of electrospinning allows for the introduction of multiple functionalities in a single step process; therefore, bi-functional scaffolds could be produced including a second functionality, the Hep peptide, on the ‘abluminal’ side of the scaffold and in direct contact with the seeded SVPs. The saphenous vein derived pericytes regulate the endothelial cell function by releasing a large array of pro-angiogenic and pro-proliferative growth factors and cytokines, which have been shown to contribute to their therapeutic action *in vivo*.<sup>[10,12]</sup> Our results showed that the Hep peptide was able to efficiently bind fluorescent heparin and to increase the retention of the SVP-produced VEGF, increasing EC adhesion and density on the scaffold. These results confirm that the conjugation of Hep to PCL does not impair its heparin binding capacity<sup>[26,29]</sup> and suggest that its localization is optimal to adsorb and release growth factors on the scaffold. Indeed, the Hep peptide provides versatile coordinating capacity for a variety of pro-angiogenic growth factors presenting a heparin-binding domain, such as VEGF, angiopoietin and fibroblast growth factor-2 (FGF-2)<sup>[33]</sup>. We hypothesize that the formation of a heparin-bound growth factor reservoir might prove advantageous *in vivo*. The transplanted SVPs would initially secrete growth factors, attracting the host endothelium

to the graft and replenishing the reservoir within the scaffold. Later, the stored growth factors might play a role in supporting the growth of host cells, after they replaced the SVPs.<sup>[6,34]</sup>

Interestingly, the proposed scaffold could represent an alternative route of delivery to harness and potentiate the therapeutic properties of the SVPs. In the context of vascular grafts, several autologous cell types have been tested to improve the clinical outcome of TEVGs, including human skeletal muscle pericytes<sup>[35]</sup> and bone marrow derived mesenchymal cells.<sup>[9]</sup> However, despite the encouraging results, cell sourcing often poses an additional burden to the patient. The SVPs can be isolated from the leftover of the saphenous vein obtained during the cardiac bypass procedure, avoiding additional harvesting procedure and providing a readily available source of therapeutic cells from the same cardiac patients that might need the synthetic grafts in the future. Furthermore, using adventitial pericytes is the more specific manner to recreate the adventitial stem cell niche. Previous studies have shown that integrity of the adventitial and perivascular layers is essential for durability of vascular grafts.<sup>[36]</sup> Our GMP-compliant SOPs for SVP isolation and expansion has now been transferred to NHS Blood and Transplant unit which is a recognized authority for cell therapy manufacture in UK. This represents a step forward to clinical use of SVPs. Accordingly, we have shown that the SVP-seeded scaffolds can be preserved in cell therapy-compatible freezing medium maintaining its functionality. Potentially, this would allow the preparation and storage of seeded TEVG as an off-the-shelf product, especially if we consider the privileged immune-modulatory phenotype of SVPs, suggesting their amenability to allogeneic transplantations.<sup>[14]</sup> Previous efforts aimed at obtaining off-the-shelf frozen cell-derived TEVG were limited to the preparation of a devitalized frozen scaffold.<sup>[37]</sup>

As previously discussed, the cells seeded on the vascular graft promote the migration and proliferation of the local endothelial cells on the scaffold surface. Indeed, the ability of SVPs to promote endothelial cell coverage was preserved on the scaffold, as demonstrated by the

increased number of endothelial cells detected in the co-culture settings.<sup>[10]</sup> Interestingly, SVPs were also able to influence endothelial cell migration, as evidenced by the increased gap closure and direct migration. In previous studies the SVPs conditioned medium showed no effect on endothelial cell migration,<sup>[10]</sup> indicating that the co-culture is a necessary condition for the release of pro-migratory factors by SVPs and supporting the beneficial effect of using SVPs in a scaffold-based approach. The effect of SVPs was increased by the presence of the peptides as demonstrated by the confluent endothelial monolayer obtained on Hep/Adh scaffolds seeded with SVPs.

In summary, we report the preparation of a pericytes-seeded, peptide-conjugated electrospun scaffold presenting two spatially distinct functionalities, which intrinsically promote endothelialisation and co-adjuvate the pro-angiogenic and pro-migratory effects of the pericytes. *In vitro*, the scaffold herein described displayed a great degree of endothelialization and a distinctive potential for rapid *in vivo* exploitation, due to its resilience to freezing, the biocompatibility of the material and the GMP quality of the cells employed. It is interesting to note that in this work we employed the well-established endothelial cell model (HUVECs) which is of foetal origin; it remains to be established if the observed effects could be even more prominent utilizing cells from an ageing donor.

We envision that the developed proof-of-concept scaffold could be implemented into a superior synthetic vascular graft, presenting both immediate and long term pro-migratory stimuli aimed at accelerating endothelialization. It is expected that the fast recruitment of endothelial cells from the neighbouring vessels solicited by the attractive presence of SVPs and the adhesive luminal surface would improve the thrombo-resistance in the short term and in the long run contribute to a reduced neointima hyperplasia thanks to the sustained release of pro-angiogenic growth factors from the reservoir created by the heparin-binding compartment.

## 4. Experimental section

### *Cell culture and co-culture conditions*

SVPs were obtained as previously described by digestion of vein leftover, obtained from cardiac bypass patients with their signed consent, as approved by the Bath Research Ethics Committee (approval number 06/Q2001/1970).<sup>[10]</sup> Briefly, venous samples were minced and digested with Liberase 2 (Roche, Basel, Switzerland). SVPs were derived from CD34positive/CD31negative cells isolated by magnetic bead–assisted cell sorting (MACS, Miltenyi).<sup>[10,12]</sup>

Both human umbilical vein endothelial cells (HUVECs, Lonza) and SVPs were cultured in endothelial growth medium (EGM2, Lonza); SVPs were seeded on gelatin and fibronectin coated plates, as previously described.<sup>[10,12]</sup>

### *Scaffold preparation and characterization*

Peptides (Hep: CGGGAAALRKKLKGA and Adh: SVVYGLRGGC) were synthesized on a Symphony Quartet peptide synthesizer (Protein Technologies, Inc., Tucson, Arizona) using standard Fmoc chemistry on the solid-phase. The crude products were purified using a reverse phase preparative high performance liquid chromatography (HPLC, Shimadzu) running a mobile phase gradient of 95% deionized water and 5% acetonitrile (ACN) to 100% ACN with 0.1% (v/v) trifluoroacetic acid (TFA). The Phenomenex C<sub>18</sub> Gemini NX column was 150 x 21.2 mm and had a 5 µm pore size. The resulting pure products were confirmed by electrospray ionization mass spectrometry (ESI-MS) (**Figure S1**). A terminal cysteine plus a glycine spacer was incorporated in the peptide design to allow for attachment to PCL.

The peptide-functionalized scaffolds were prepared following a previously established protocol.<sup>[17]</sup> In brief, to first prepare the polymer-peptide conjugates, the terminal hydroxyl groups of PCL (MW14 kDa) were modified with a heterobifunctional linker p-maleimidophenyl isocyanate (PMPI) to generate maleimide-functionalized PCL. Then, the modified PCL was dissolved in DMF with either the Hep or Adh peptide, and allowed to react overnight in the presence of a few drops of DIPEA. The resulting conjugates were washed extensively with water to remove unbound peptide and peptide attachment was confirmed by nuclear magnetic resonance (NMR, **Figure S2**). Fluorescently labelled conjugates were obtained by reacting the available amines of the peptide with either fluorescein isothiocyanate (FITC) or NHS-rhodamine in DMF with a few drops of DIPEA. Next, 1% (w/v) Hep- and Adh-PCL was blended with 11% (w/v) unmodified PCL (MW 80 kDa) in 1,1,1,3,3,3-hexafluoro-2-propanol (HFIP) and electrospun either as a single peptide mats (CTL, Hep or Adh) or as a dual peptide scaffold (Adh/Hep). Scanning electron microscopy (SEM) was used to verify the fiber size and the scaffold architecture.

Scaffolds were electrospun on a custom built device as previously reported.<sup>[38]</sup> Briefly, the electrospinning device consisted of a faraday cage (Phnoenix Mechano Limited, UK), two high voltage sources (ETPS Limited, UK), and two syringe pumps (NE-1010 High Pressure Syringe Pump, World Precision Instruments, UK), providing a constant polymer flow through the needle (blunt needle, 18G Terumo, Scientific Laboratory Supplies Ltd, Wilford, UK). The positive voltage was applied to the needle, whereas the collector was on a negative bias. High voltage was controlled by a custom made software based on labview (Empa, Swiss Federal Laboratories of Materials Science and Technology, St. Gallen, Switzerland) via a labjack interface (labjack, RS components, UK). All mono-functionalised scaffolds and control scaffolds were spun at 11/-5kV, 2mL·h<sup>-1</sup> flow rate and a distance of 11 cm. Bi-functional scaffolds (Adh/Hep) were produced with a modified method, employing two

syringe pumps combining the two polymers via teflon tubing and a three way valve. By this, continuous spinning without changing syringes or polymer solutions could be guaranteed and bi-functional scaffolds were not subjected to delamination.

Fibre diameter was measured with ImageJ software, based on SEM images, for each condition, 50-100 fibres were measured.

Scaffolds were sterilized in 70% (v/v) ethanol for 30 minutes and incubated with 1% (w/v) bovine serum albumin for 3 hours prior to further applications.

#### *Peptide functionality on the scaffold*

To assess the binding of heparin, 12 mm discs were cut out from the different scaffolds and incubated with 5 µg/ml of heparin-FITC (Life Technologies) overnight at room temperature and then thoroughly washed. For VEGF binding, SVPs were seeded at 70% confluence and transfected with 0.5 µg of plasmid encoding for VEGF165 tagged with GFP (RG229662, OriGene), using Fugene at 3:1 ratio (Promega). After 6 hours transfection medium was removed and replaced with EGM2 (Lonza) and the transfected cells were incubated with different PCL scaffolds for 48 hours. Expression of the transgene was verified by qPCR, using QuantStudio 6 Real time PCR (LifeTechnologies) and the following primers: F-AGGGCAGAATCATCACGAAT and R-AGGGTCTCGATTGGATGGCA (**Figure S3**). Binding of fluorescent proteins to the scaffolds was quantified by fluorescence microscope imaging. Three images of each scaffold were taken at 4x with the same camera setting and quantified as mean grey value (mean fluorescence) using FIJI software. This measure is linearly correlated to the fluorescent protein concentration (**Figure S4**).

For the functional characterization of VEGF binding to control and Hep scaffolds, 8mm round scaffolds were cut and incubated for 2 hours at 37C with heparin (100µg/ml) and VEGF (200µg/ml) or just heparin as control. After a 30 min wash,  $1 \times 10^5$  HUVECs were

plated on each scaffold in EBM medium containing 0.5% (v/v) FBS. AlamarBlue® was performed as described above at 48 hours.<sup>[39]</sup>

To test the influence of peptide functionalization on endothelial coverage,  $1 \times 10^5$  HUVECs were seeded on each 8mm scaffold for 48h. Scaffolds were then fixed, stained with Wheat Germ Agglutinin-AlexaFluor 488 (WGA-488) and DAPI and 4 imaged (4x) of each scaffold were obtained and quantified. Higher magnification pictures (10x and 20x) were used as representative images.

#### *Co-culture on PCL scaffolds*

To test the cumulative effect of the peptides and the SVPs co-culture, control and Hep/Adh scaffolds were cut in 18 mm discs, locked in 24 well plate CellCrown™ (Sigma) inserts, and  $1.5 \times 10^5$  Wheat Germ Agglutinin-AlexaFluor 568 (WGA-568) stained SVPs were seeded and let to attach for 2 hours on the Hep side. Then,  $2.5 \times 10^5$  WGA-488 stained HUVECs were seeded on the Adh side by inverting the scaffold inside the CellCrowns™. Cells were cultured for 48 hours and then fixed and stained with DAPI. Number of nuclei was counted in three random fields acquired at 4x, using FIJI (ImageJ). Each experiment included at least two biological replicates and was repeated three independent times; each experiment was normalized to the control (control PCL without SVPs).

For gap closure experiment, a modification of the protocol above was applied wherein the  $1.5 \times 10^5$  SVPs and  $7.5 \times 10^5$  HUVECs were seeded on 6 well plate CellCrown™. Prior to HUVECs seeding a 0.5 mm PDMS barrier was locked in the middle of the PCL mat to prevent adhesion of the endothelial cells in the central region. After 3 hours, non-adherent HUVECs were washed away and the barrier was removed. Migration into the gap was assessed at 48 hours by fluorescence imaging of the whole well and quantified as mean grey value in 10 random fields of the gap area (n=3).



### *Transwell migration assay*

Prior to the start of migration,  $1.5 \times 10^4$  SVPs were seeded on each well of a 24 well plate in 500  $\mu$ l of complete medium overnight. Transwell® inserts (Corning, 8  $\mu$ m pores) were coated with fibronectin on the lower side and  $5 \times 10^4$  HUVECs were added to the upper chamber and let migrate for 8 hours. Next, remaining cells in the upper chamber were removed and cells migrated to the lower side of the transwell were fixed, stained with DAPI and counted. Five random fields were imaged at 4x for each four biological replicates; the results are normalised to the spontaneous migration values. The average of seven independent experiments is reported.

### *Scaffold freezing and recovery*

Hep/Adh scaffolds were cut in 14 mm discs and seeded with  $1.5 \times 10^5$  SVPs. After 24 hours half of the samples were frozen in CTST™ Synth-a-Freeze® Cryopreservation Medium (LifeTechnologies), a GMP manufactured, chemically defined, protein-free freezing medium and half underwent AlamarBlue® measurement, as described above. After 14 days, frozen scaffolds were recovered in full medium for 24 hours and then tested with AlamarBlue® in the same conditions used for the controls. Results were normalized to the fluorescence value of AlamarBlue® incubated with unseeded scaffolds. After measurement cells were fixed and stained with WGA-488.

To test the post-freezing functionality, recovered scaffolds were inserted in CellCrown™ supports and 50,000 WGA-488 stained HUVECs were plated on the ‘luminal’ side of each scaffold. The number of adherent HUVECs was quantified after 48 hours.

### *Statistical analysis*

Each experiment was repeated 3-7 independent times (N) and 2-4 technical replicates (n) were included within each repeat. Data were analysed using GraphPad Prism 5 and are expressed as mean  $\pm$  SD. For pairwise comparison, unpaired t-test was performed. For multiple comparisons, one-way ANOVA was performed, followed by Bonferroni post-test. A  $P < 0.05$  was considered significant.

### Supporting Information

Supporting Information is available from the Wiley Online Library or from the author.

### Acknowledgements

We would like to thank Dr A. Serio for his help with the imaging.

This work was supported by a Whitaker International Scholarship to A.J.G. and J.L.P., while M.M.S., L.W.C. and J.L.P. gratefully acknowledge support from the Medical Research Council, the Engineering and Physical Sciences Research Council and the Biotechnology and Biological Sciences Research Council UK Regenerative Medicine Platform Hub “Acellular Approaches for Therapeutic Delivery” (MR/K026682/1). M.M.S. also acknowledges the support from the ERC Seventh Framework Programme Consolidator grant “Natura CG” under grant agreement no. 616417. The work on the pericytes isolation and scale up was supported by the Medical Research Council (MRC MR/J015350/1) and Heart Research UK grants. A.G.G. has been funded by a Fellowship from the Swiss National Science Foundation SNF, Grant No. P2BEP3\_152091 and P300PB\_161072. The authors acknowledge Empa, Swiss Federal Laboratories for Materials Science and Technology, St. Gallen, Switzerland for providing the electrospinning software and helping with device setup.

The raw data for reproducing figures presented in the paper can be found at DOI: 10.5281/zenodo.157186.

Received: ((will be filled in by the editorial staff))

Revised: ((will be filled in by the editorial staff))

Published online: ((will be filled in by the editorial staff))

### References

- [1] A. Ratcliffe, *On the occasion of the XVII Meeting of the FECTS 2000*, 19, 353.
- [2] K. A. Rocco, M. W. Maxfield, C. A. Best, E. W. Dean, C. K. Breuer, *Tissue Eng Part B Rev* **2014**, 20, 628.
- [3] A. Hasan, A. Memic, N. Annabi, M. Hossain, A. Paul, M. R. Dokmeci, F. Dehghani, A. Khademhosseini, *Acta Biomater* **2014**, 10, 11.
- [4] M. A. Cleary, E. Geiger, C. Grady, C. Best, Y. Naito, C. Breuer, *Trends Mol Med*

**2012**, *18*, 394.

- [5] S. Kaushal, G. E. Amiel, K. J. Guleserian, O. M. Shapira, T. Perry, F. W. Sutherland, E. Rabkin, A. M. Moran, F. J. Schoen, A. Atala, S. Soker, J. Bischoff, J. E. J. Mayer, *Nat Med* **2001**, *7*, 1035.
- [6] J. D. Roh, R. Sawh-Martinez, M. P. Brennan, S. M. Jay, L. Devine, D. A. Rao, T. Yi, T. L. Mirensky, A. Nalbandian, B. Udelsman, N. Hibino, T. Shinoka, W. M. Saltzman, E. Snyder, T. R. Kyriakides, J. S. Pober, C. K. Breuer, *Proc Natl Acad Sci U S A* **2010**, *107*, 4669.
- [7] C. K. Hashi, Y. Zhu, G.-Y. Yang, W. L. Young, B. S. Hsiao, K. Wang, B. Chu, S. Li, *Proc Natl Acad Sci U S A* **2007**, *104*, 11915.
- [8] T. Shinoka, G. Matsumura, N. Hibino, Y. Naito, M. Watanabe, T. Konuma, T. Sakamoto, M. Nagatsu, H. Kurosawa, *The Journal of Thoracic and Cardiovascular Surgery* **2005**, *129*, 1330.
- [9] N. Hibino, E. McGillicuddy, G. Matsumura, Y. Ichihara, Y. Naito, C. Breuer, T. Shinoka, *The Journal of Thoracic and Cardiovascular Surgery* **2010**, *139*, 431.
- [10] P. Campagnolo, D. Cesselli, A. Al Haj Zen, A. P. Beltrami, N. Krankel, R. Katare, G. Angelini, C. Emanuelli, P. Madeddu, *Circulation* **2010**, *121*, 1735.
- [11] R. G. Katare, P. Madeddu, *Trends Cardiovasc Med* **2013**, *23*, 66.
- [12] R. Katare, F. Riu, K. Mitchell, M. Gubernator, P. Campagnolo, Y. Cui, O. Fortunato, E. Avolio, D. Cesselli, A. P. Beltrami, G. Angelini, C. Emanuelli, P. Madeddu, *Circ. Res.* **2011**, *109*, 894.
- [13] E. Avolio, M. Meloni, H. L. Spencer, F. Riu, R. Katare, G. Mangialardi, A. Oikawa, I. Rodriguez-Arabaolaza, Z. Dang, K. Mitchell, C. Reni, V. V. Alvino, J. Rowlinson, U. Livi, D. Cesselli, G. Angelini, C. Emanuelli, A. P. Beltrami, P. Madeddu, *Circ Res* **2015**, *116*, e81.
- [14] H. Domev, I. Milkov, J. Itskovitz-Eldor, A. Dar, *Stem Cells Translational Medicine* **2014**, *3*, 1169.
- [15] S. G. Wise, M. J. Byrom, A. Waterhouse, P. G. Bannon, A. S. Weiss, M. K. C. Ng, *Acta Biomater* **2011**, *7*, 295.
- [16] E. Pektok, B. Nottelet, J.-C. Tille, R. Gurny, A. Kalangos, M. Moeller, B. H. Walpoth, *Circulation* **2008**, *118*, 2563.
- [17] L. W. Chow, A. Armgarth, J.-P. St-Pierre, S. Bertazzo, C. Gentilini, C. Aurisicchio, S. D. McCullen, J. A. M. Steele, M. M. Stevens, *Adv Healthc Mater* **2014**, *3*, 1381.
- [18] S. T. Barry, S. B. Ludbrook, E. Murrison, C. M. T. Horgan, *Experimental Cell Research* **2000**, *258*, 342.
- [19] Y. Yokosaki, N. Matsuura, T. Sasaki, I. Murakami, H. Schneider, S. Higashiyama, Y. Saitoh, M. Yamakido, Y. Taooka, D. Sheppard, *J. Biol. Chem.* **1999**, *274*, 36328.
- [20] Y. Hamada, K. Nokihara, M. Okazaki, W. Fujitani, T. Matsumoto, M. Matsuo, Y. Umakoshi, J. Takahashi, N. Matsuura, *Biochem. Biophys. Res. Commun.* **2003**, *310*, 153.
- [21] Y. Lei, O. F. Zouani, M. Rémy, C. Ayela, M.-C. Durrieu, *PLoS ONE* **2012**, *7*, e41163.
- [22] K. M. Park, Y. Lee, J. Y. Son, J. W. Bae, K. D. Park, *Bioconjugate Chem.* **2012**, *23*, 2042.
- [23] Y. Hamada, K. Yuki, M. Okazaki, W. Fujitani, T. Matsumoto, M. K. Hashida, K. Harutsugu, K. Nokihara, M. Daito, N. Matsuura, J. Takahashi, *Dent Mater J* **2004**, *23*, 650.
- [24] S. Kale, R. Raja, D. Thorat, G. Soundararajan, T. V. Patil, G. C. Kundu, *Oncogene* **2014**, *33*, 2295.
- [25] H. Egusa, Y. Kaneda, Y. Akashi, Y. Hamada, T. Matsumoto, M. Saeki, D. K.

- Thakor, Y. Tabata, N. Matsuura, H. Yatani, *Biomaterials* **2009**, *30*, 4676.
- [26] K. Rajangam, H. A. Behanna, M. J. Hui, X. Han, J. F. Hulvat, J. W. Lomasney, S. I. Stupp, *Nano Lett.* **2006**, *6*, 2086.
- [27] K. Rajangam, M. S. Arnold, M. A. Rocco, S. I. Stupp, *Biomaterials* **2008**, *29*, 3298.
- [28] L. W. Chow, R. Bitton, M. J. Webber, D. Carvajal, K. R. Shull, A. K. Sharma, S. I. Stupp, *Biomaterials* **2011**, *32*, 1574.
- [29] L. W. Chow, L.-J. Wang, D. B. Kaufman, S. I. Stupp, *Biomaterials* **2010**, *31*, 6154.
- [30] L. Ye, X. Wu, H.-Y. Duan, X. Geng, B. Chen, Y.-Q. Gu, A.-Y. Zhang, J. Zhang, Z.-G. Feng, *J Biomed Mater Res A* **2012**, *100*, 3251.
- [31] W. Zheng, Z. Wang, L. Song, Q. Zhao, J. Zhang, D. Li, S. Wang, J. Han, X.-L. Zheng, Z. Yang, D. Kong, *Biomaterials* **2012**, *33*, 2880.
- [32] A. N. Lyle, G. Joseph, A. E. Fan, D. Weiss, N. Landazuri, W. R. Taylor, *Arterioscler. Thromb. Vasc. Biol.* **2012**, *32*, 1383.
- [33] P. Chiodelli, A. Bugatti, C. Urbinati, M. Rusnati, *Molecules* **2015**, *20*, 6342.
- [34] T.-N. Tsai, J. P. Kirton, P. Campagnolo, L. Zhang, Q. Xiao, Z. Zhang, W. Wang, Y. Hu, Q. Xu, *Am. J. Pathol.* **2012**, *181*, 362.
- [35] W. He, A. Nieponice, L. Soletti, Y. Hong, B. Gharaibeh, M. Crisan, A. Usas, B. Peault, J. Huard, W. R. Wagner, D. A. Vorp, *Biomaterials* **2010**, *31*, 8235.
- [36] M. D. Guillemette, R. Gauvin, C. Perron, R. Labbe, L. Germain, F. A. Auger, *Tissue Eng Part A* **2010**, *16*, 2617.
- [37] W. Wystrychowski, T. N. McAllister, K. Zagalski, N. Dusserre, L. Cierpka, N. L'Heureux, *J Vasc Surg* **2014**, *60*, 1353.
- [38] A. G. Guex, A. Frobert, J. Valentin, G. Fortunato, D. Hegemann, S. Cook, T. P. Carrel, H. T. Tevæarai, M. N. Giraud, *Acta Biomater* **2014**, *10*, 2996.
- [39] A. G. Guex, G. Fortunato, D. Hegemann, H. T. Tevæarai, M.-N. Giraud, in *Stem Cell Nanotechnology*, Humana Press, Totowa, NJ, **2013**, pp. 119–131.

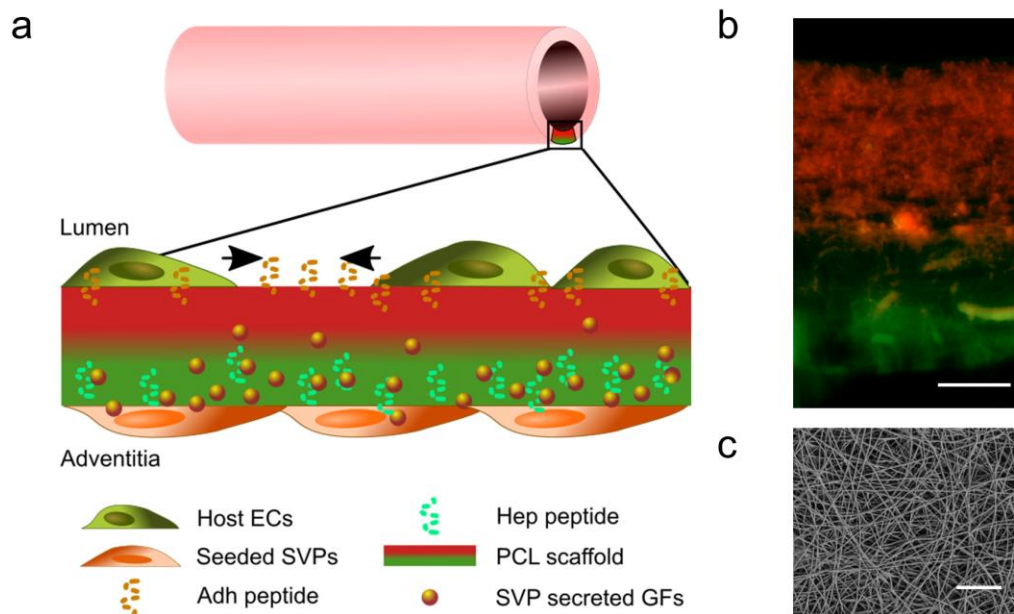


**Figure 1. Characterization of the engineered scaffold for blood vessel graft applications.**

The bifunctional scaffold is composed of electrospun peptide-conjugated polycaprolactone (PCL) fibres seeded on the abluminal side with patient-derived pro-angiogenic saphenous vein pericytes (SVPs).

As shown in the schematic (a) and the overlaid fluorescence microscopy image (b), the luminal side of the scaffold is mainly decorated with the Adh peptide (in red), to increase host endothelial cell (ECs) adhesion, migration and spreading. The outer layer presents mainly the Hep peptide (in green), which binds and present the SVP-produced growth factors (GFs). SEM image showing the size and distribution of the fibres in the scaffold (top view, c). Scale bars: 50 μm.

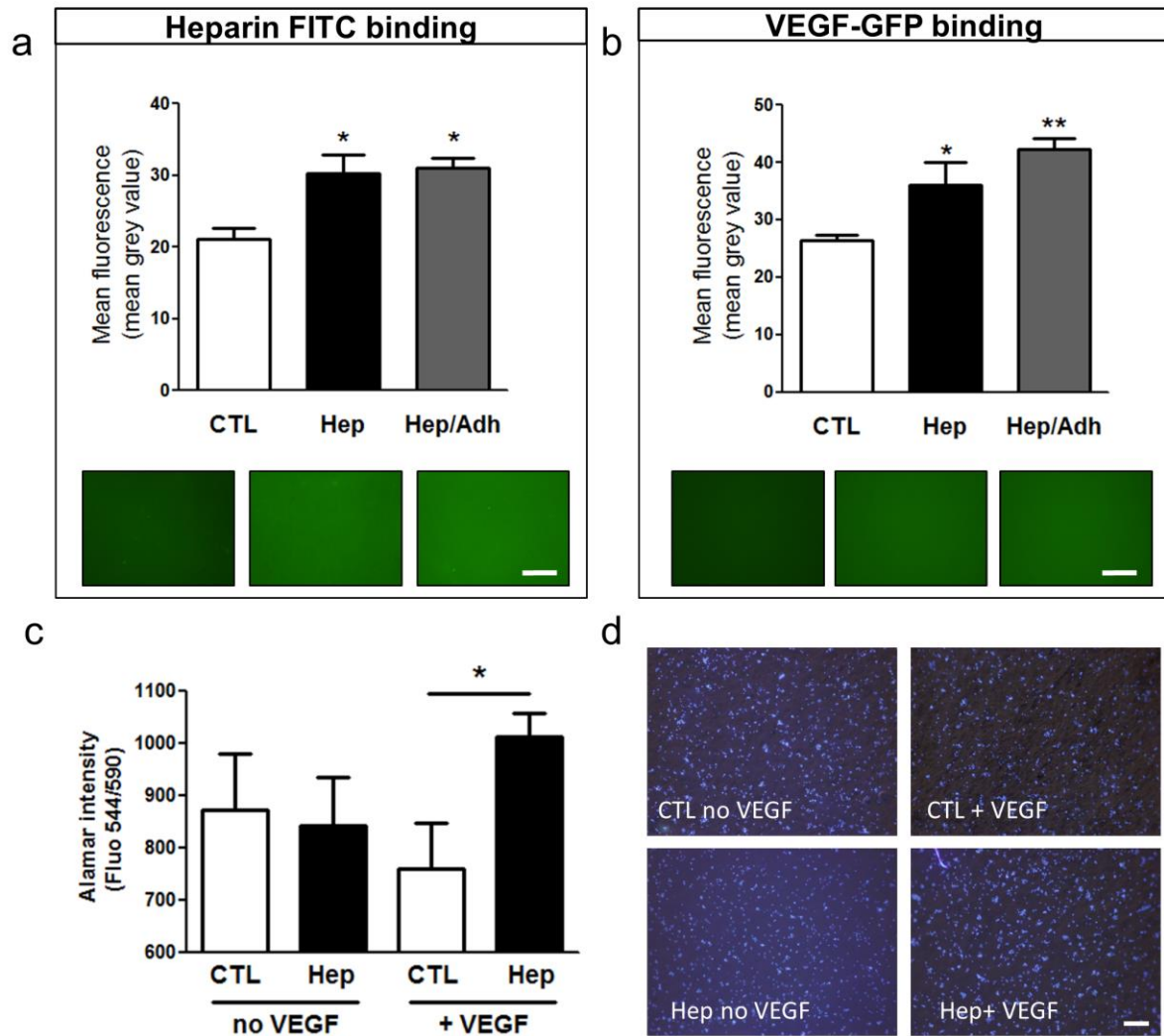


**Figure 2. Hep peptide binds and coordinates SVP-produced growth factors.** Mean fluorescence (mean grey value) measuring the binding of heparin-FITC (a) and SVP-secreted VEGF-GFP (b) to unconjugated (CTL), Hep-conjugated (Hep) and dual peptide (Hep/Adh) scaffolds. Alamar blue (c) and representative images (d) show the increased HUVEC growth on VEGF loaded Hep mats. \* $P < 0.05$ , \*\* $P < 0.01$ . Scale bars: 500  $\mu\text{m}$ .  $N = 3$ ;  $n = 3$ .

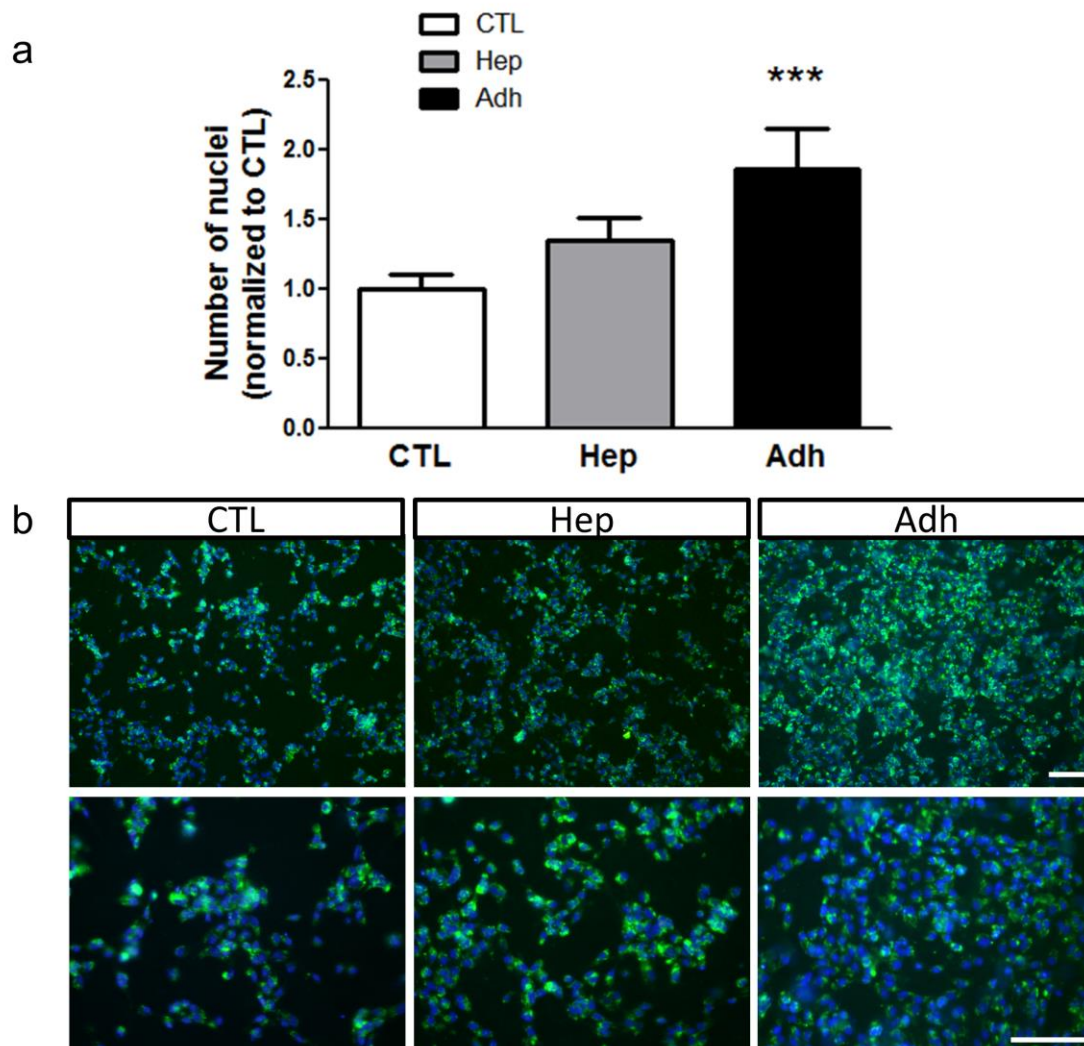


**Figure 3. Adh peptide specifically increases endothelial cell adhesion and growth.**

HUVECs were seeded on electrospun PCL scaffolds either unconjugated (CTL) or functionalised with Hep or Adh peptides. Cell density was measured at 48 hours post-seeding and is expressed as fold change over CTL (a, N = 4; n = 2). Representative images showing endothelial coverage on the different scaffolds (green: WGA-488, blue: DAPI, b).

\*\*\*P<0.001. Scale bars: 100  $\mu$ m.

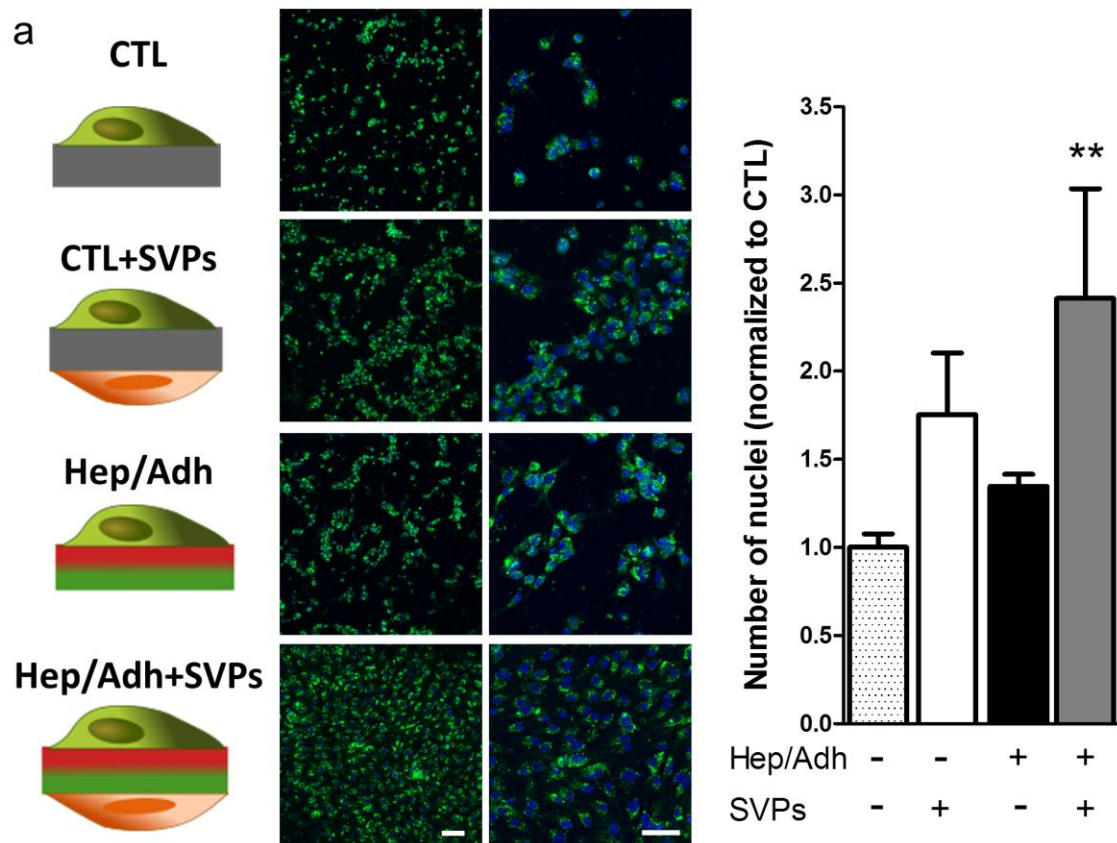


**Figure 4. The combination of bifunctional scaffold and SVP seeding increases endothelial coverage.** Fluorescently labelled HUVECs were seeded on plain PCL (CTL) or dual peptide scaffolds (Hep/Adh), in presence or absence of pericytes (SVPs). Representative confocal micrographs showing the resulting coverage in each condition (a; green: WGA-488; blue: DAPI). Number of nuclei quantified at 48 hours is shown as a ratio over the control (b; plain PCL, no SVPs; N = 3; n = 2). \*\*P<0.01 vs. CTL. Scale bar: 100  $\mu$ m.



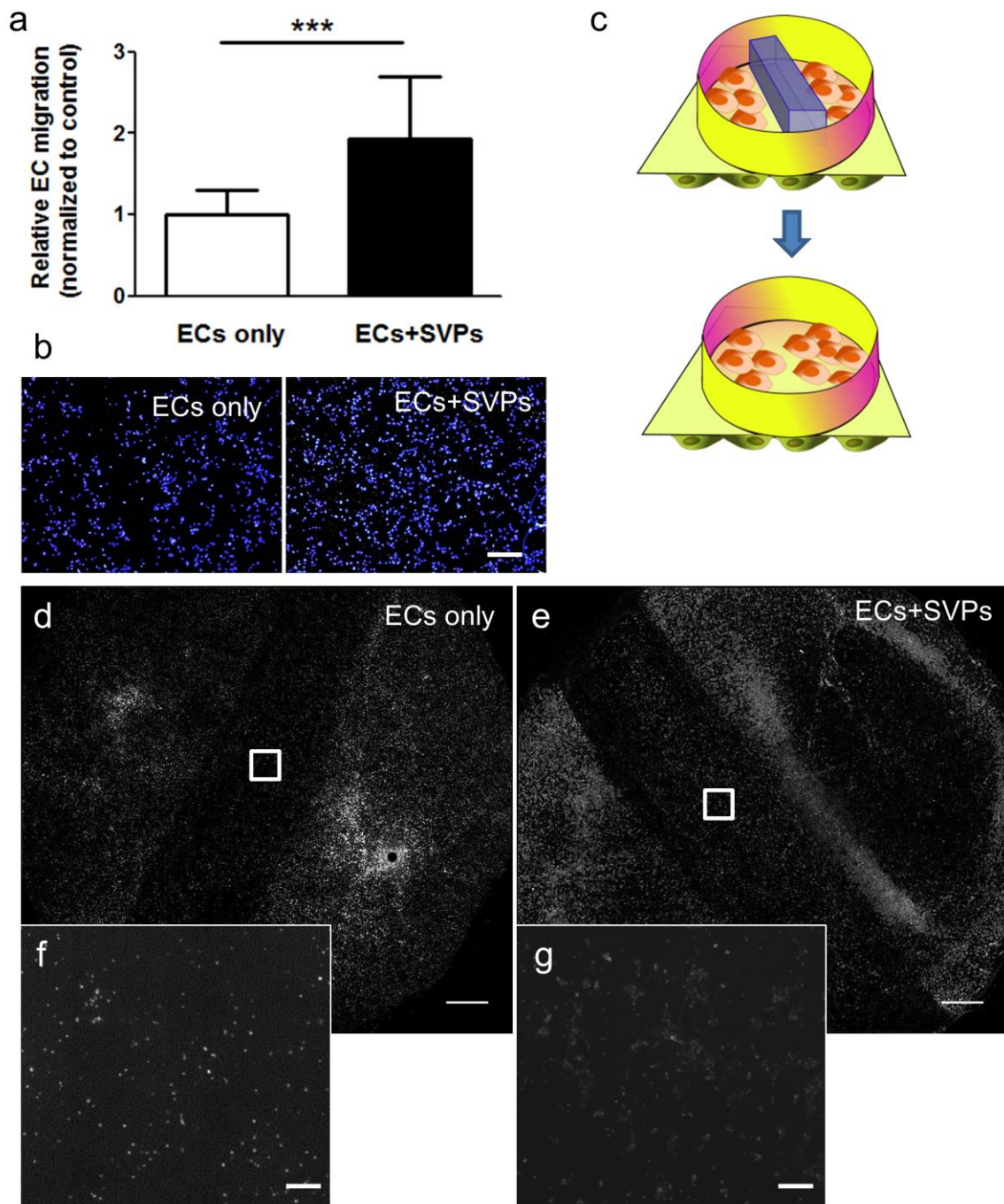


**Figure 5. Seeding of SVPs induces EC migration and gap closure.** In a transwell™ migration assay, the seeding of SVPs (ECs+SVPs) in the lower chamber induces EC migration, as compared to EC spontaneous migration (ECs only). Relative migration quantification (a) and representative pictures are shown (b, blue: DAPI; N = 7; n = 4). The Hep/Adh scaffold was secured in a CellCulture™ crown, after seeding with SVPs on the

lower side (ECs+SVPs) and a barrier was placed in the middle to prevent HUVEC adhesion and create a gap. HUVECs were plated on the top chamber and the barrier was removed to allow their migration (c). Gap closure was monitored at 48 hours, showing that seeding of the SVPs on the lower side of the scaffold promotes HUVEC gap invasion (d-g; grey scale: WGA-488; N=3). \*\*\*P<0.001. Scale bars: 400  $\mu$ m (b, f and g) and 2 mm (d and e).

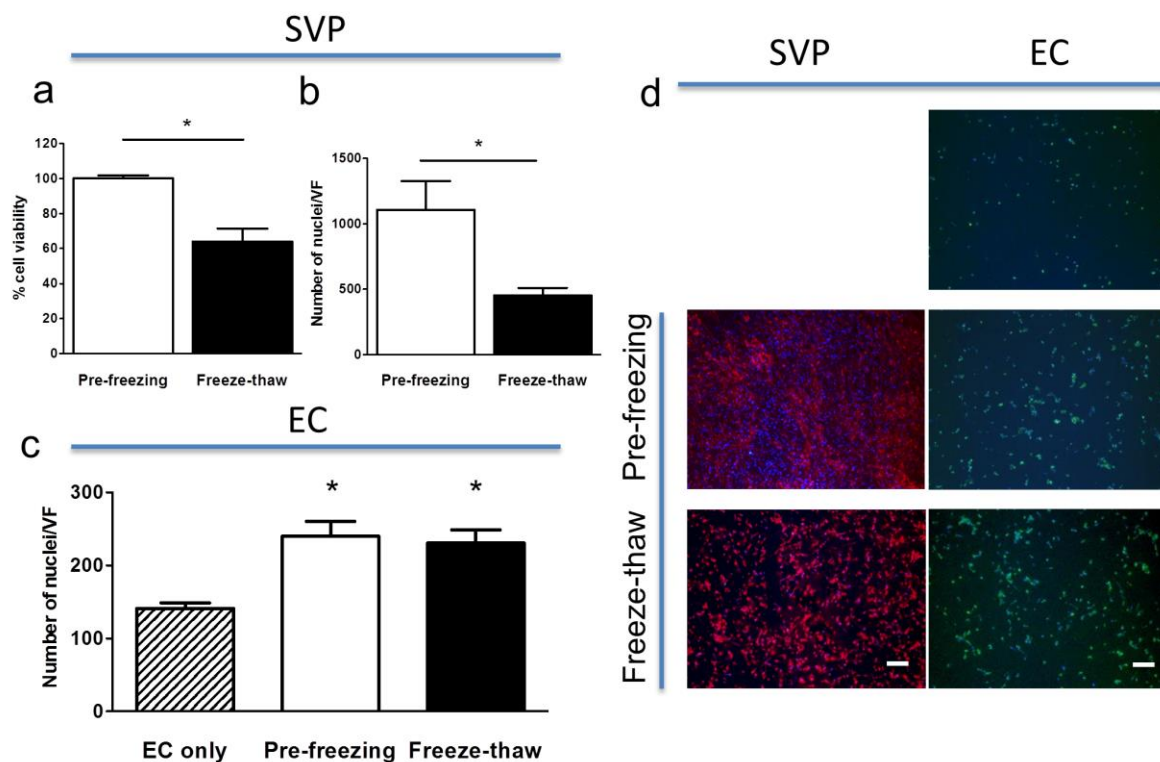


**Figure 6. Freezing of SVP-seeded PCL preserves cell viability and function.** SVP seeded grafts were frozen and recovered, preserving over 65% viability (a) and 50% cell confluency (b). Freeze-thawed SVP were equally able to promote EC density, as compared to freshly plated SVP (c). SVP after the freeze and thaw process remain adherent to the scaffold (d, red: WGA-568) and promoted EC density (d, green: WGA-488). \*P<0.05. Scale bars: 200  $\mu$ m. N = 3.